CHAPTER IV
PREPARATION OF POLYBENZOXAZINE-DERIVED PARTIALLY ORDERED CARBON

· 4.1 Abstract

Partially ordered carbons have been widely studied and used in various applications such as catalyst supports, and electrode materials. They have been conventionally prepared by pyrolysis and physical or chemical activation of organic precursors such as polymers, in which the pore size and pore structure, can be controlled at a high temperature in inert atmosphere. In this study, the solventless process was used to prepare polybenzoxazine precursor, which was synthesized from formaldehyde, phenol and aromatic diamine to produce partially ordered carbon with high chair yield. The effects of the pyrolysis temperatures on the microstructure of the obtained partially ordered carbons were investigated. The change in the chemical structure of polybenzoxazine was examined by FTIR and TGA was used to investigate thermal properties. The physical properties were examined by SAA. In addition, XRD was used to demonstrate the characteristics of d spacing in partially ordered carbon. The electrical property of partially ordered carbon was observed at room temperature by an electrometer with two-point probe.

4.2 Introduction

Many researchers have discovered and studied carbons which are graphite, graphene and carbon nonotube were attracted in electronic applications because their properties such as thermal stabillity and conductivity. Graphene is a single carbon layer of graphite structure, describing its nature by analogy to a polycyclic aromatic hydrocarbon of quasi-infinite size as according to the IUPAC definition from 1995. Graphene is the subset of graphite, carbon nanotubc and fullerene [1]. In this material, carbon atoms are arranged in a regular hexagonal pattern. It is a one-atom thick layer of the layered mineral graphite. This two-dimensional material constitutes a new partially ordered carbon including layers of carbon atoms forming six-membered rings [2]. Ideally graphene is a single-layer material, but graphene samples with two or more layers are being investigated with equal interest. Graphenes can be defined in to three different types: single-layer graphene (SG), bi-layer graphene (BG) and few-layer graphene (number of layers $\leq$ 10). Graphene exhibits large specific surface area and unique electrical, mechanical and thermal properties [2-6]. It shows excellent physical and chemical properties, which makes it promising for variety of applications in the areas such as solar-cells, energy storage, field effect transistors, catalyst support, sensors, and nanocomposites [7-12].

The first preparation of single-layer graphene was reported by Novoselov and coworker [3]. In 2007, Black and coworker reported the direct chemical exfoliation of graphite into graphene without a graphene oxide step [13]. The first preparation of graphite oxide was achieved by oxidative treatment of graphite by employing Hummers procedure [14] A chemical method to prepare single-layer graphene involves reduction of single-layer graphene oxide dispersion in dimethlyformamide with hydrazine hydrate [15], or sodium and ethanol [16]. At the same time, single-layer graphene have been exfoliated in N-methylpyrrolidone [17] or a surfactant/water solution using ultrasonication [18]. Besides, chemical vapor deposition was used to prepare single-layer graphene by decomposing a variety of hydrocarbons on films or sheets, the number of layers varying with the hydrocarbon and reaction parameters of transition metal [19]. The thermal exfoliation of graphitic oxide is an important method to prepare few-layer graphene at high temperatures

[20-21]. Another method of preparing few-layer graphene is by reacting single-layer graphene oxide in water with hydrazine hydrate at the refluxing temperature [22] or by microwave treatment [23]. The effect of heating nanodiamond at different temperatures has been studied by Enoki and coworker [24-25]. Annealing of nanodiamond at high temperatures in an inert atmosphere produces few-layer graphenes [21, 26].

The preparations of conductive carbon, almost transform of graphite to graphene, are complicated and expensive process. Therefore, novel carbons have been developed including partially ordered carbon. It has been widely studied and used in various applications such as atmosphere separation, catalyst supports, and electrode material. It has been conventionally prepared by pyrolysis and physical or chemical activation of organic precursors such as polymers in which the pore size and pore structure can be controlled during the process at very high temperature in inert atmosphere. Polybenzoxazine as a novel developed class of thermosetting resins derived from phenolic resin. It possesses various good properties like high thermal stability, easy processability and very high char yield. A method for preparing a desired benzoxazine compound comprises preparing a substantially homogeneous reaction mixture that includes a phenolic compound, a primary amine and an aldehyde. It has been synthesized from inexpensive raw materials and polymerized by a ring-opening addition reaction [27-28]. The ways of producing benzoxazine monomer based on the functional group of reactants. They are mono-functional, di-functional and multifunctional group [29]. Because of the benzoxazine monomer are resuting in linear and branch structure. It may cause reduce the properties of benzoxazine. In 2005, Takeichi and colleague synthesized high molecular weight polybenzoxazine precursors from aromatic or aliphatic diamine and bisphenol-A with paraformaldehyde [30].

The present work has been synthesized benzoxazines precursors based on aniline, methylenedianiline and tetraethylenepentamine in ordered to study the changing ordered structure of partially ordered carbon. Benzoxazines precursors were polymerized to be polybenzoxazine and then pysolyzed to obtain ￩partially ordered carbon, Heat treatment, is varous pysolyzed temperatures, has been used to enhance the ordered structure of partially ordered carbon. Moreover, silver nitrate

was loaded in benzoxazine precursor in ordered to improve the thermal and electrical properties of partially ordered carbon. Finally, polybenzoxa-zine and partially ordered carbon were characterized to study their properties.

4.3 Experimental

4.3.1 Materials

All chemicals were used without further purification. The benzoxazines was synthesized using various types of amine; aniline (99%) was purchased from Panreac Company, 4,4'-methylenedianiline (≥97%), paraformaldehyde powder (95%) and tetraethylenepentamine (95%) were purchased from Sigma-Aldrich Co., Ltd and Phenol detached crystals (99.99%) was obtained from Fisher Chemical company. Silver nitrate was used to enhance thermal properties of benzoxazines and purchased from VRBIOSCIENCE Co., Ltd.

4.3.2 Measurements

The functional groups related to structure of materials were investigated by using FTIR technique. The FT-IR spectra were obtained using a Nicolet Nexus 670 FT-IR spectrometer in the frequency range of 400-4000 cm^{-1} with 64 scans at a resolution of 2 cm^{-1}. KBr pellet technique was applied in the preparation of powder samples. DSC analyzer was carried out using a Perkin-Elmer DSC 7 instrument. The sample was heated from 50 to 300 °C with heating rate 10 °C per minute under N_2 atmosphere with flow rate 20 ml per minute. Finally, the heating profile, curing temperature and completely cured polybenzoxazine were obtained. TGA instrument was also conducted with Perkin Elmer Thermogravimetric /Differential Thermal Analyzer (TG-DTA). The sample was loaded in rang 4-8 mg on the alumina pan and heated from 50 to 800 °C under nitrogen atmosphere with flow rate 50 ml per minute and heating rate 10 °C per minute. The pyrolyzed temperature of polybenzoxazine was investigated from the onset temperature whereas char yield as the weight residue at 800 °C was reported. The X-ray powder diffraction pattern of the carbon foam was obtained using an XRD (Bruker AXS D8 ADVANCE) spectrometer with Cu Kα irradiation (λ = 0.15406 nm) at 40 kV and

30mA to examine the graphitization of the partially ordered carbon after carbonization. Surface area analyzer (SAA) was used to determined surface area, pore volume and pore size distribution of activated carbon. The results were obtained by Quantachrome/Autosorb-1 based on the Brunauer-Emmett-Teller (BET) and Barret-Joyner-Halenda (BJH) using nitrogen adsorption isothermal at 77 K. The sample wasloaded around 0.2 g and removed atmosphere at 250 °C. The electrical conductivity values of the partially ordered carbons were obtained by measuring the resistances and calculate the electrical conductivity. The geometric correction factor was determined by calibrating the four-point probe with semi-conducting silicon sheets of known resistivity values. Applied dc currents were small to be in the linear Ohmic regime. The electrical conductivity of the partially ordered carbon was observed at room temperature by an electrometer with two-point probe (Keithley model 6517A)

4.3.3 Methodology

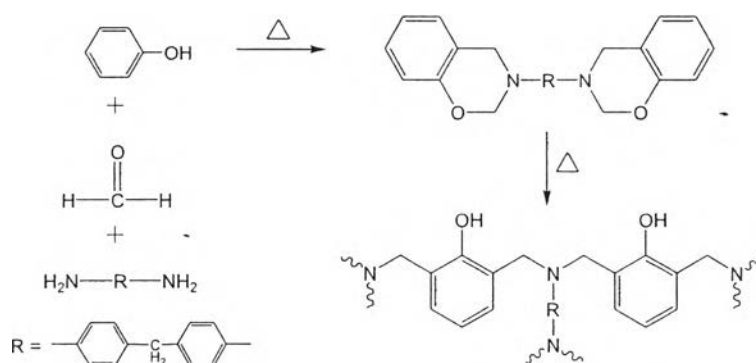#### 4.3.3.1 Synthesis of Aniline-based Polybenzoxazine (PBZ-A)

The solventless method invented by Ishida [27] was used to synthesize benzoxazine prepolymer with a mole ratio of phenol: aniline: paraformaldehyde is 1: 1: 2. The mixtures of phenol, paraformaldehyde and aniline were heated at 100 °C until they change to be transparent yellow viscous. From this step, aniline-based benzoxazine precursor (BZ-A) was obtained. Before curing step, the benzoxazine precurcers were grinded and then cured at 240 °C for 1 h in ambient air. Finally, aniline-based polybenzoxazine will be obtained.
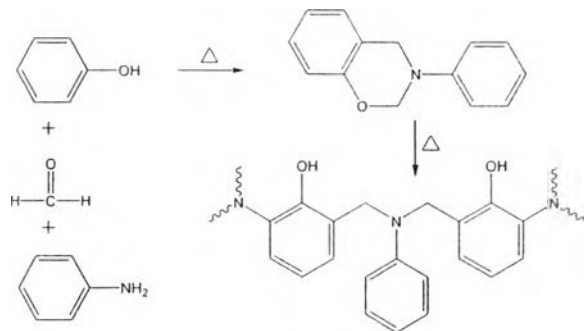
Scheme 4.1 Synthesis of aniline-based polybenzoxazine.

4.3.3.2 Synthesis of Methylenedianiline-based Polybenzoxazine (PBZ-MDA)

The mixtures of phenol, paraformaldehyde and methylene-dianiline with ratio 2: 4: 1 were heated at 100 °C until they change to be transparent yellow viscous. From this step, methylenedianiline-based benzoxazine precursor (BZ-MDA) was obtained. Before curing step, the benzoxazine precurcers were grinded and then cured at 230 °C for 1 h in ambient air. Finally, methylenedianiline-based polybenzoxazine will be obtained.

Scheme 4.2 Synthesis of methylenedianiline-based polybenzoxazine.

4.3.3.3 Synthesis of Tetraethylenepentamine-based Polybenzoxazine (PBZ-TEPA)

The mixtures of phenol, paraformaldehyde and tetraethylene-pentamine with ratio 2: 4: 1 were heated at 100 °C until they change to be transparent yellow viscous. From this step, tetraethylenepentamine-based benzoxazine precursor (BZ-TEPA) was obtained. Before curing step, the benzoxazine precurcers were grinded and then cured at 250 °C for 1 h in ambient air. Finally, tetraethylene pentamine-based polybenzoxazine will be obtained.
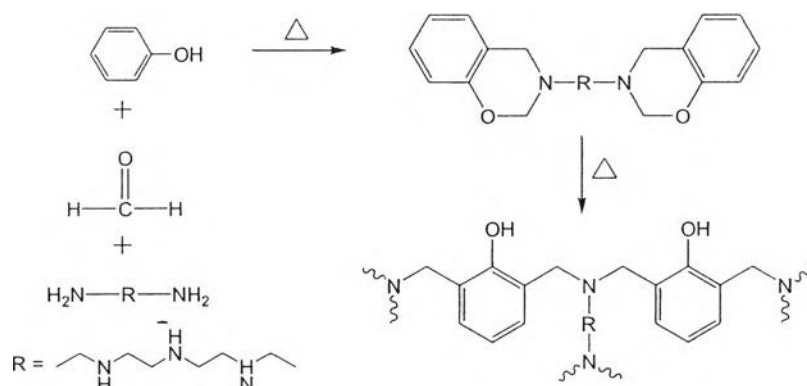
Scheme 4.3 Synthesis of tetraethylenepentamine-based polybenzoxazine.

4.3.3.4 Synthesis of Methylenedianiline-based Polybenzoxazine with Silver Nitrate (PBZ-MDA- AgNO₃)

The methylenedianiline-based benzoxazine precursor that was obtained from previous step and silver nitrate were mixed together with weight ratio 10: 1. The mixtures were heated at 100 °C until they change to be homogeneous brown viscous. Before curing step, the benzoxazine precurcers were grinded and then cured at 220 °C for 1 h in ambient air. Finally, methylenedianiline-based polybenzoxazine with silver nitrate will be obtained.

4.3.3.5 Preparation of Partially Ordered Carbon by Pysolysis (NC)

Fully cured polybenzoxazines base on various types of amine were pyrolyzed at 500, 800 and 120 °C with heating rate 2 °C per minute and under N_2 with flow rate 500 cm³ per minute. Partially ordered carbons have been obtained after the temperature goes to room temperature. Partially ordered carbons base on aniline, methylene-dianiline and tetraethylenepentamine were abbreviated to NC-A, NC-MDA and NC-TEPA respectively. For activated carbons base on methylenedianiline with silver nitrate were abbreviated to NC-MDA-AgNO₃.

4.3.3.6 Preparation of Activated Carbon (AC)

Obtained partially ordered carbons by pyrolysis were activated at 900 °C for 3 h under CO_2 with flow rate 500 cm³ per minute. Partially ordered carbons have been obtained after the temperature goes to room temperature. Activated carbons base on methylenedianiline was abbreviated to AC-MDA.

4.3.3.7 Characterization of Polybenzoxazine and Partially Ordered Carbon

The effects of the pyrolysis temperatures on the micro-structure of the obtained partially ordered carbon have been investigated. The changing in chemical structures of polybenzoxazine was examined by FTIR. Moreover, TGA was used to investigate the thermal properties. The physical properties of the products were also investigated by SAA. In addition, XRD was used to demonstrate the characteristics d spacing of the resulting partially ordered carbon. The electrical property of partially ordered carbon was observed at room temperature by an electrometer with two-point probe (Keithley model 6517A)

4.4 Results and discussions

4.4.1 The Physical Structure of Polybenzoxazines and Partially Ordered Carbon

Figure 4.1 shows photography of bulk polybenzoxazine and partially ordered carbon based on MDA were obtained by pyrolysis at 800 °C. As seen in the figure, the partially ordered carbon based on MDA exhibits a swollen non-uniform foam-like structure underneath a glittering skin layer. As expected for a typical foaming process, atmospherees generated during decomposition of the bulk polybenzoxazine have expanded the polybenzoxazine into a swollen foam-like structure as the same with previous research [32].
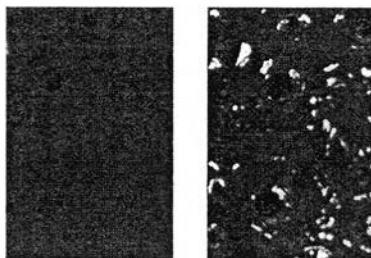

Figure 4.1 Photographs of bulk polybenzoxazine (left) and partially ordered carbon based on MDA were obtained by pyrolysis at 800 °C (right).

4.4.2 <u>The Chemical Structure of Benzoxazine Precursors and Polyben-</u>
<u>zoxazines</u>

4.4.2.1 The Chemical Structure of Aniline-based Benzoxazine Precursors and Polybenzoxazines

Aniline-based polybenzoxazine have been synthezied by solventless method as well as MDA-based and TEPA-based polybenzoxazine. The chemical structure of benzoxazine precursors and benzoxazine were investigated by FTIR technique. The FTIR spectra of benzoxazine precursors and benzoxazine were shown in Figure 4.2-4.4. Figure 4.2 shows the FTIR spectra of Aniline-based benzoxazine precursor and the polybenzoxazine. The characteristic absorption bands of benzoxazine precursor emerge at 680 and 740 cm^{-1} for C-H bending and ring puckering. The symmetric stretching of C-O-C shows at 833, 941, 1003 and 1373 cm^{-1}. The bands at 1157 and 1219 cm^{-1} demonstrate the stretching of C-N-. For the stretching of aromatic C=C appears at 1481 and 1589 cm^{-1}[31]. The C-O-C bands of fully cured polybenzoxazine disappear and generate the broad band of -OH group after the step cure. These results are corresponding with the study of Takeichi [30], suggesting that the peak disappearance is due to the ring-opening polymerization of the benzoxazine precursors.

4.4.2.2 The Chemical Structure of TEPA-based Benzoxazine Precursors and Polybenzoxazines

The FTIR spectra of TEPA-based benzoxazine precursor and the polybenzoxazine were shown in Figure 4.3. The characteristic absorption bands of benzoxazine precursor emerge at 757 and 811 cm^{-1} for C-H bending and ring puckering. The symmetric stretching of C-O-C presents at 872, 899, 1003 and 1345 cm^{-1}. The bands at 1099, 1138 and 1250 cm^{-1} demonstrate the stretching of C-N-. For the stretching of aromatic C=C appears at 1485, 1585 and 1664 cm^{-1}. The C-O-C bands of fully cured polybenzoxazine disappear and generate the broad band of -OH group after the step cure due to the ring-opening polymerization of the benzoxazine precursors.
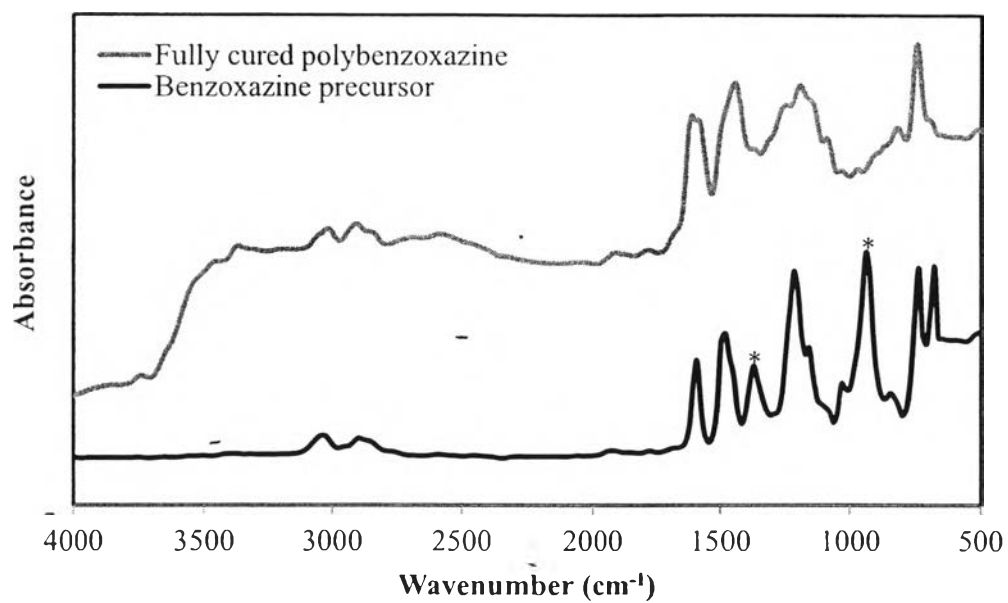
Figure 4.2 FTIR spectra of Aniline-based benzoxazine precursor and the polybenzoxazine.
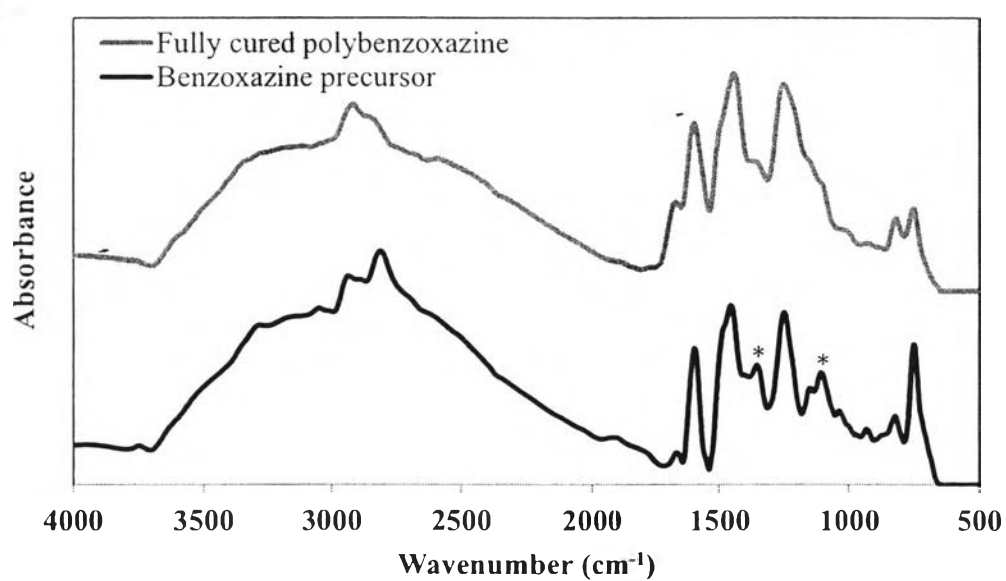

Figure 4.3 FTIR spectra of TEPA-based benzoxazine precursor and the polybenzoxazine.

4.4.2.3 The Chemical Structure of MDA-based Benzoxazine Precursors and Polybenzoxazines

Figure 4.4 shows the FTIR spectra of MDA-based benzoxazine precursor and the polybenzoxazine. The characteristic absorption bands of benzoxazine precursor emerge at 748 and 802 cm^{-1} for C-H bending and ring puckering. The absorption bands at 903, 1016 and 1358 cm^{-1} relate to the symmetric stretching of C-O-C. The bands at 1103-1218 cm^{-1} demonstrate the stretching of C-N-. For the stretching of aromatic C=C appears at 1444-1645 cm^{-1}. The C-O-C bands of fully cured polybenzoxazine disappear and generate the broad band of -OH group after the step cure due to the ring-opening polymerization of the benzoxazine precursors.
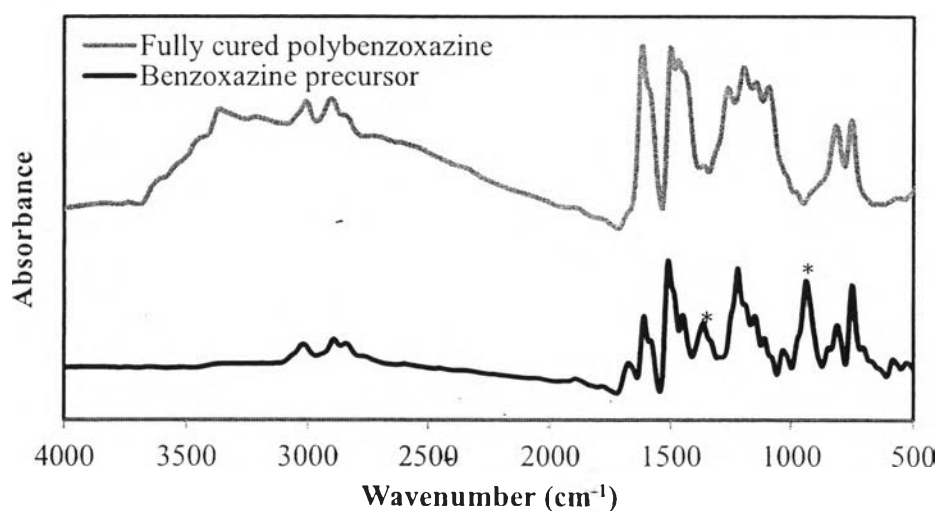

Figure 4.4 FTIR spectra of MDA-based benzoxazine precursor and the poly-benzoxazine.

4.4.2.4 The Chemical Structure of Partially Ordered Carbon

The partially ordered carbon from bulk polybenzoxazine at various pyrolysis temperatures were examined by FTIR, as shown in Figure 4.5. Evidently, the partially ordered carbon obtained from bulk polybenzoxazine reveal similar typical FTIR characteristic absorption peaks, i.e., 750 cm^{-1} (mono-substituted benzene ring), 1200 cm^{-1} (C-N-C asymmetric deformation), 1460-1480 (tetra-

substituted benzene ring), and 1550-1600 (C=C unsaturated aromatics, C=N unsaturated heterocycle) [30, 33-35]. A decrease in the intensity of all organic absorption peaks was clearly observed, when the pyrolysis temperature was increased from 500 to 1200 °C, specifically, at pyrolysis temperatures higher than 800 °C, two asymmetric broad absorption bands extending from 1000 to 1600 cm^{-1} can be observed [45-47]. It can be seen in the figure that the two bands from the pyrolyzed at 500 °C have more intensity than those pyrolyzed temperature. These bands are generally known to reflect the coalescence of the vibrational modes of C=N, C-N, and C=C bonds [36-38]. The presence of this band is strongly supports the chemical composition of the polybenzoxazine having nitrogen incorporated into a Mannich bridge within its structure. Moreover, the partially ordered carbon, was obtained from pyrolysis at 1200 °C, showed significantly increasing intensity at 1080 cm^{-1} which related the increase of C-C single bond due to the transforming partially ordered carbon.

4.4.3 Thermal Properties of Benzoxazine Precursors and Polybenzoxazines

4.4.3.1 Thermal Properties of Benzoxazine Precursors

Benzoxazine precursors were heated to produce polyben-zoxazine by the ring opening polymerization of oxazine ring. DSC technique has been used in ordered to obtain the curing temperatures of polybenzoxazine. The DSC thermogram shows the exothermal peaks and the midpoint curing temperature as shown in Figure 4.6 and concluded in Table 4.1. The curing temperature of BZ-MDA decreases about 20 °C with adding AgNO$_3$ because it is thermal conductive materials which allow the electron can flow through these materials due to their free electrons. The fully cured polybenzoxazines were achieved after have been heated for 1 h corresponding with the completely disappeared exothermal peaks of poly-benzoxazine as shown in Figure 4.7. It was similar result that reported by Takeichi and coworker [30]. The PBZ-TEPA having more nitrogen atoms in the molecules and stronger H-bonding needed a greater amount of energy for the ring opening polymerization, leading to the shift of the exothermic peak to higher temperatures —
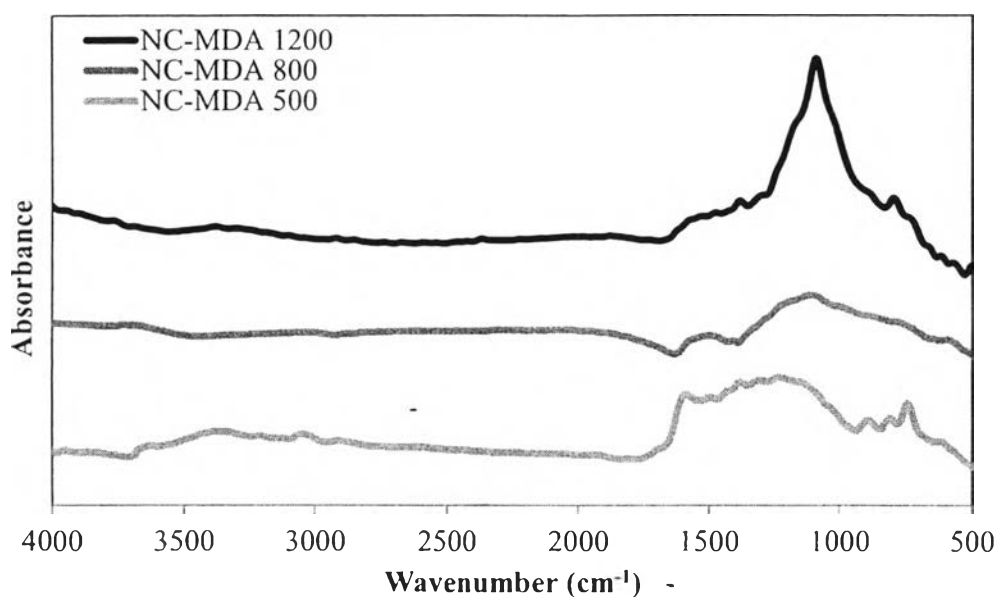
Figure 4.5 FTIR spectra of partially ordered carbon based on MDA were obtained by pyrolysis at 500, 800 and 1200 °C.

because their strong inter- and intra-hydrogen bonding when compared with PBZ-MDA and PBZ-Aniline [39]. Despite the aforementioned advantages of polybenzoxazines, the crosslinking densities of their networks are considered to be rather low because of intensive hydrogen bonding restricting segmental mobility and hence hindering network extension. For aniline-based benzoxazine, the benzene ring that is attached to the nitrogen atom has delocalized electrons, causing the electron cloud around the nitrogen atom to be lower compared to the cyclohexyl group. Thus, the nitrogen atom of the PBZ-Aniline compound should have weaker hydrogen bonding to the O-H groups compared to PBZ-TEPA. However, in the hydrogen bonded structure, the nitrogen will have a partial positive charge, and in the case of aniline-based polybenzoxazine, the delocalized electrons in the benzene ring can stabilize the nitrogen and thus the hydrogen bond is more stable in the PBZ-Aniline [40-41]. The PBZ-Aniline is mono-functional benzoxazines typically result to a linear or branched structure with a low molecular weight on the ordered of 500-2000 Da [42]. Thus, mono-functional benzoxazine monomers are precursors for

polybenzoxazine show limited usefulness as structural materials. However, they might be useful as reactive diluents to facilitate the processing [43].
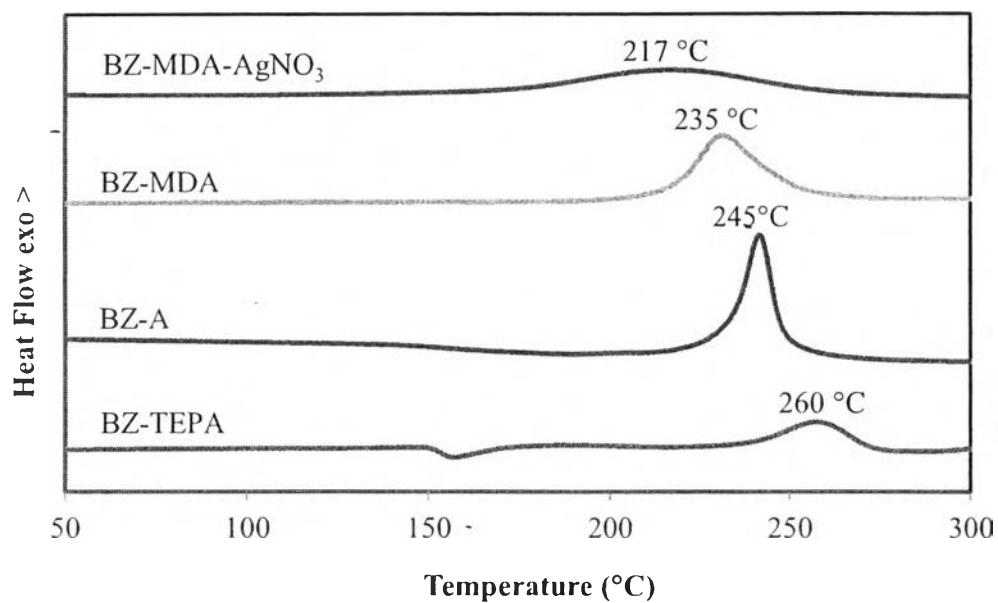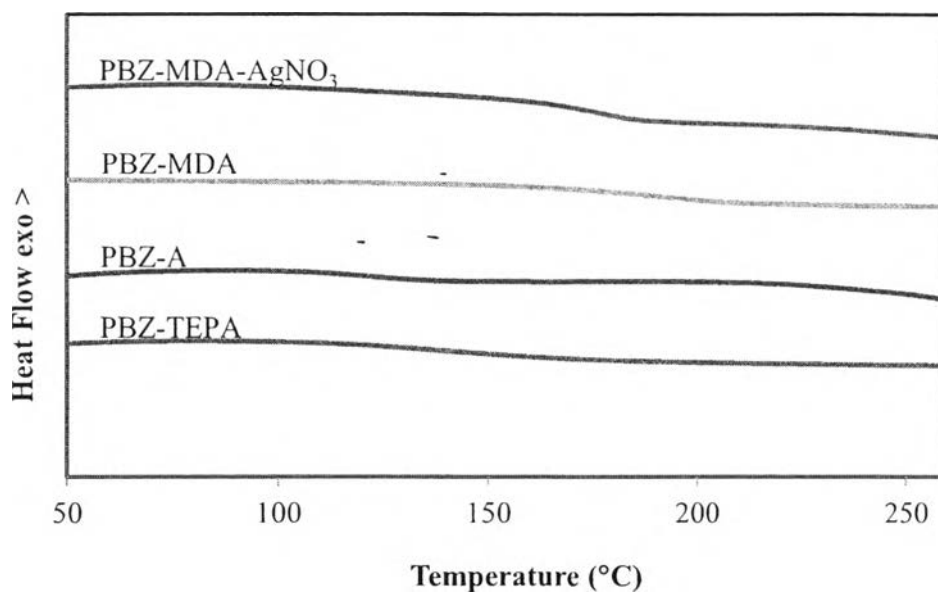

Figure 4.6 DSC thermograms of benzoxazine precursors.

Figure 4.7 DSC thermogram of fully cured polybenzoxazine.

Table 4.1 The curing temperatures of benzoxazine precursors

Benzoxazine precursor	Curing temperature (°C)
BZ-TEPA	260
BZ-A	245
BZ-MDA	235
BZ-MDA-AgNO$_3$	217

4.4.3.2   Thermal Properties of Polybenzoxazines

The expection of the increasing devolatilization with temperature was repored by Lu and colleagues [44]. The weight loss is mainly due to the drying and devolatilization upon heating in an inert atmosphere. It is seen that the weight loss increases with temperature which indicate that the yield of the char decreases with increasing temperature. The thermal properties of polybenzoxazine were examined by TGA technique under nitrogen atmosphere. The TGA thermogram was shown in Figure 4.8 and shows the decomposition temperatures or onset temperatures in ordered to relate the pyrolyzed temperature that was used to transform polybenzoxazine to carbon. The decomposition temperatures and char yields at 700 °C were summarized in Table 4.2. As can be seen, TEPA-based polybenzoxazines achieve the lowest char yield because they almost compose of aliphatic parts which we could not obtain the char. Moreover, the onset temperature of PBZ-MDA was higher than PBZ-A due to the diaromatic amine of MDA-based polybenzoxazine.

Table 4.2 The decomposition temperatures polybenzoxazines

Polyenzoxazine	Onset temperature (°C)	Char yield (%)
PBZ-TEPA	240	20
PBZ-A	322	46
PBZ-MDA	356	46
PBZ-MDA-AgNO$_3$	345	56

However, its char yield as same as the PBZ-A. This is because A- and MDA-based polybenzoxazine are slightly different structure. The decomposition temperature of PBZ-MDA decreased around 10 °C with loading $AgNO_3$ because $AgNO_3$ is thermal conductive material which can induce the heart to surround materials. As a result of adding 10 wt% $AgNO_3$, the char yield of $AgNO_3$-loaded PBZ-MDA increased 10% from unloading $AgNO_3$.
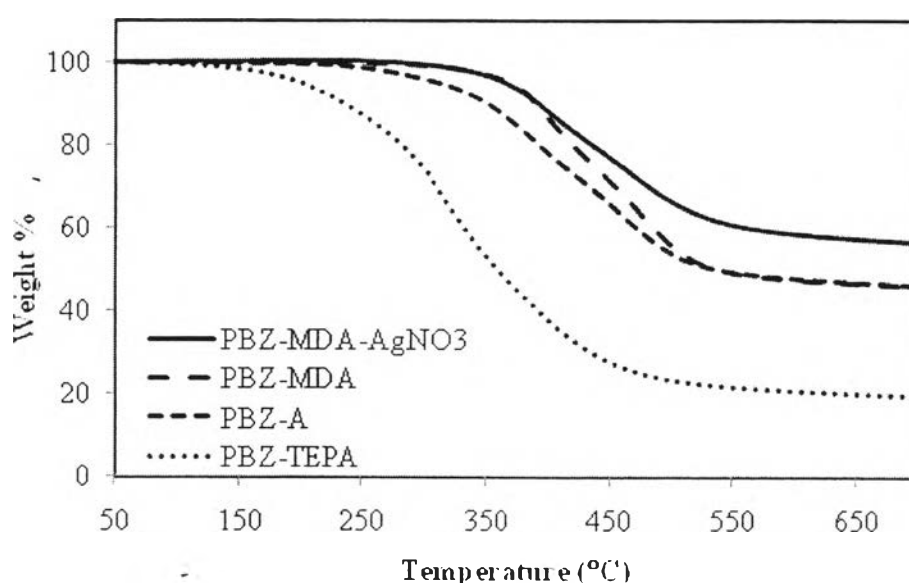

Figure 4.8 TGA thermogram of polybenzoxazines.

4.4.4 Crystalline Structure of Partially ordered carbon

4.4.4.1 The Crystalline Structure of Activated Carbon and Partially Ordered Carbon derived from MDA-based Polybenzoxazine

Partially ordered carbons have been prepared from fully cured poly-benzoxazine though the pyrolysis at 500, 800 and 1200 °C with heating rate 2 °C per minute and under N_2 with flow rate 500 cm^3 per minute. To consider the crystalline structure of partially ordered carbon, the XRD technique was used to carry out the reflection peaks as shown in Figure 4.9. The XRD pattern of the partially ordered carbons shows broad peaks at $2\theta = 23°$, $43°$ and $80°$. The d-spacing, calculated by Bragg's equation, corresponds to the interlayer spacing (d_{002}) and the

stacking height ($L_{c,002}$) of graphitic carbon material [45-49]. Their diffraction peaks as accordance with the turbostratic structure [50]. The located diffraction peaks at 43° arise from the ordereding of C atoms inside the graphene layers. The graphene layers within a turbostratic structure can be considered as individual two-dimensional crystallites built up of hexagonal two-dimensional unit cells and with the in-plane size equal to the layer diameter. The maximum corresponding to the diffraction peaks at 23° shows that graphene sheets are already formed and organised as parallel layers spaced at a relatively well-defined interplanar distance (d_{002}) [51].

Following the pyrolyzed temperture at 500, 800 and 1200 °C all resulting conductive materials are of amorphous state by appearing of any broad peaks recorded in their X-ray diffractograms. Their foreign atoms such as oxygen and nitrogen were completely disappeared from polybenzoxazine with increasing pyrolyzed temperature. Especially, the pyrolyzed temperture at 1200 °C results in entire graphitization of the materials and decreases the diffraction peaks at 23° due to either more packing of interplanar or less interplanar distance. Moreover, the diffraction peaks of the partial graphite were appeared when the pyrolyzed temperature of activated carbon up to 800 °C. The increase of the diffraction peaks at 43° causes to reduce the turbostratic structure. Thus, the polymers go through crystal structure changes towards the crystal structure of graphite as the pyrolysis temperature increases as the in Figure 4.9-4.10 [52].

4.4.4.2 The Crystalline Structure of Partially Ordered Carbon derived from Various Types Amine Polybenzoxazine and Pyrolyzed at 500 and 800 °C

The x-ray diffractograms of partially ordered carbon derived from various types of amine and pyrolyzed at 500 °C were shown in Figure 4.11. The partially ordered carbon derived from A- and TEPA-based polybenzoxazine show less ordered than MDA- based polybenzoxazine with correspond the diffraction peaks at 23°. Due to the chemical structure of aniline-based polybenzoxazine was prepared mono-functional benzoxazines typically result to a linear or branched structure with a low molecular weight on the ordered of 500-2000

Da [42]. and TEPA-based polyben zoxazine was aliphatic structure which is less ordered structure and transformed to lowest partially ordered carbon due to the result

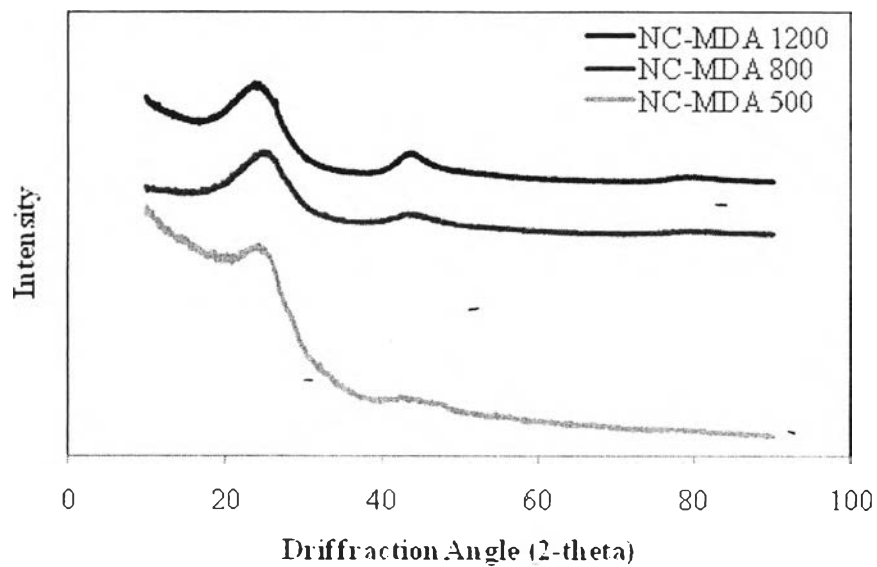**Figure 4.9** XRD spectra of partially ordered carbon derived from MDA-based poly-benzoxazine with various pyrolyzed temperature.
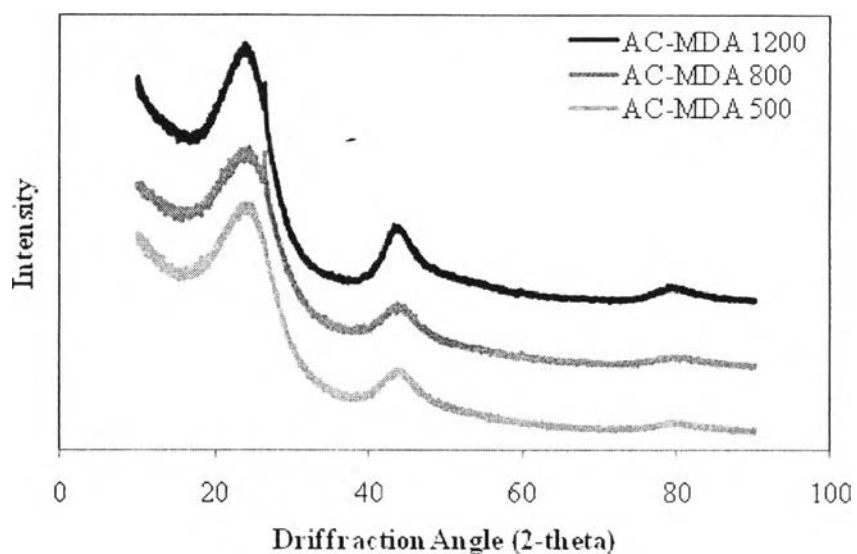

Figure 4.10 XRD spectra of activated carbon derived from MDA-based polybenzoxazine with various pyrolyzed temperature.
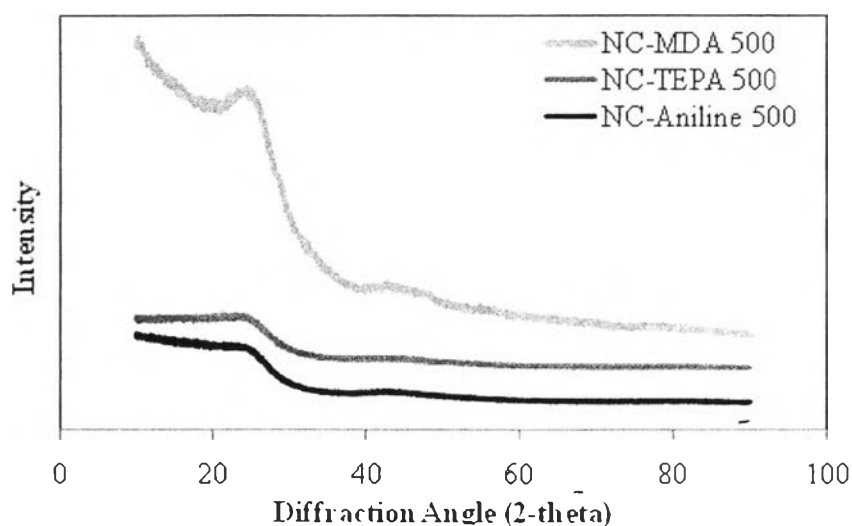
Figure 4.11 XRD spectra of partially ordered carbon derived from various types of amine and pyrolyzed at 500 °C.

from aliphatic structure. Moreover, the aliphatic structure in TEPA has a long chain, its tranforming of chain can not pack well. In ordered to obtain char yield, the chemical structure must be six member ring or aromatic. The MDA- based polybenzoxazine showed higher ordered because of its aromatic. The increased intensities of all partially ordered carbon derived from various types of amine and pyrolyzed at 800 °C resulting in the diffraction peaks at 23° increased as shown in Figure 4.12 owing to increase the pyrolyzed temperature.

According to this XRD characterization, it can be inferred that the resulting carbon prepared in this study was partially crystalline, but had less crystallinity than graphite. Moreover, the ordered structure of these carbons significantly increases with temperature. Especially, the partially ordered carbons derived from MDA-based polybenzoxazine exhibited the significantly increasing ordered structure due to the promoting of theirs chemical structures which consist of the packing of aromatic of phenol and MDA.
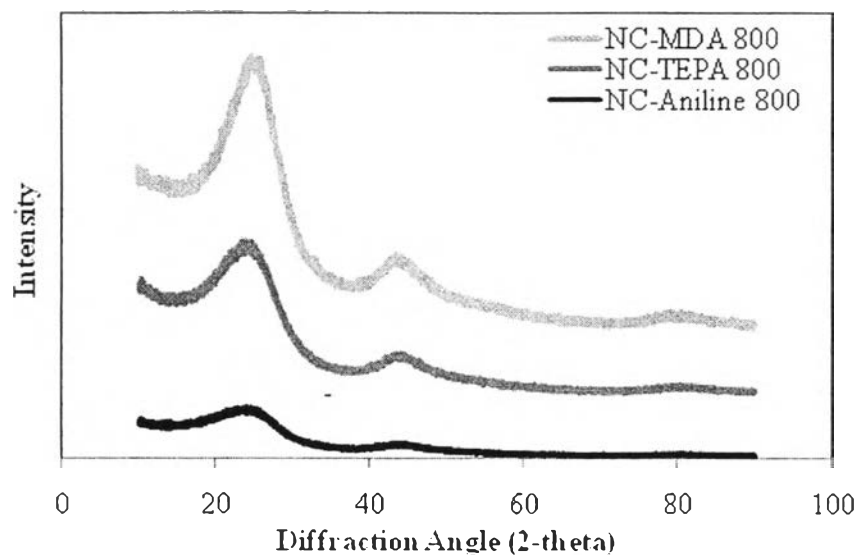
Figure 4.12 XRD spectra of partially ordered carbon derived from various types of amine and pyrolyzed at 800 °C.

4.4.5 Surface Area Analysis of Partially Ordered Carbon and Activated Carbon

The characteristics of pore structure of partially ordered carbon and activated carbon such as surface area, total pore volume and average pore diameter were investigated by adsorption and desorption nitrogen and outatmosphere sample at 250 °C and summarized in Table 4.3. The BET surface area of both partially ordered carbon and activated carbon increases and pore diameter decreases with increasing pyrolyzed temperature from 500 to 800 °C because the formation of small pores for the removal of light molecules and atmospherees during pyrolysis [47]. In case of activated carbon, the pore diameters are similarly size because carbon dioxide atmosphere acts ac weak acid and erodes the surface of partially ordered carbon. When the pyrolyzed temperature is over 800 °C causing in the decrease of surface area could be due to the shrinkage of the pores and packing of carbon [53]. Moreover, the increasing of pore diameter due to the creating larger pore from the shrinkage of small pore and a higher temperature causes micropores to widen because it destroys the walls between adjacent pores [54].

The activated carbon showed the significantly increasing surface area and total pore volume comparing with partially ordered carbon. The activation of partially ordered carbon with CO_2 must have involved the $C-CO_2$ reaction [55]. This would lead to the removal of carbon atoms and also cause the burn-off, therefore contributing to the development of micropore structure. Two effects which are volatile material loss and $C-CO_2$ reaction tend to increase micropore volume and surface area [56].

Table 4.3 Characteristics of pore structure of partially ordered carbon and activated carbon

Chemical	Surface area (m^2/g)	Total pore volume (cm^3/g)	Micropore volume (cm^3/g)	Micropore fraction (%)	Average pore diameter (nm)
NC-MDA 500	12.06	1.16×10^{-2}	2.96×10^{-3}	26	3.84
NC-MDA 800	48.72	1.58×10^{-2}	4.60×10^{-3}	29	1.30
NC-MDA 1200	6.34	6.62×10^{-3}	1.61×10^{-3}	24	4.18
AC-MDA 500	321.00	1.74×10^{-1}	1.67×10^{-1}	96	2.17
AC-MDA 800	466.20	2.48×10^{-1}	2.43×10^{-1}	98	2.13
AC-MDA 1200	25.44	2.57×10^{-2}	9.03×10^{-3}	35	4.04

4.4.6 The Electrical Conductivities of Partially Ordered Carbon and Activated Carbon

The electrical conductivities of partially ordered carbon and activated carbon with various pyrolyzed temperature as shown in Figure 4.12. In case of partially ordered carbon, the electrical conductivities increased greatly with increasing the pyrolyzed temperature from 500 to 800 °C and continuously increased when the pyrolyzed temperature has risen to 1200 °C [52, 57-60]. This is the electrical conduction mechanism is the hopping of carriers through the carbon "island" to the next aromatic ring [52]. Moreover, the pyrolysis goes continuously at higher temperature with a continuous network of aromatic rings creates within an amorphous carbon matrix which is formed due to a progressive carbonization among the ring systems and enhances the size of the conductive fused rings allowing electric current to flow longer distances within the individual conductive species [57].
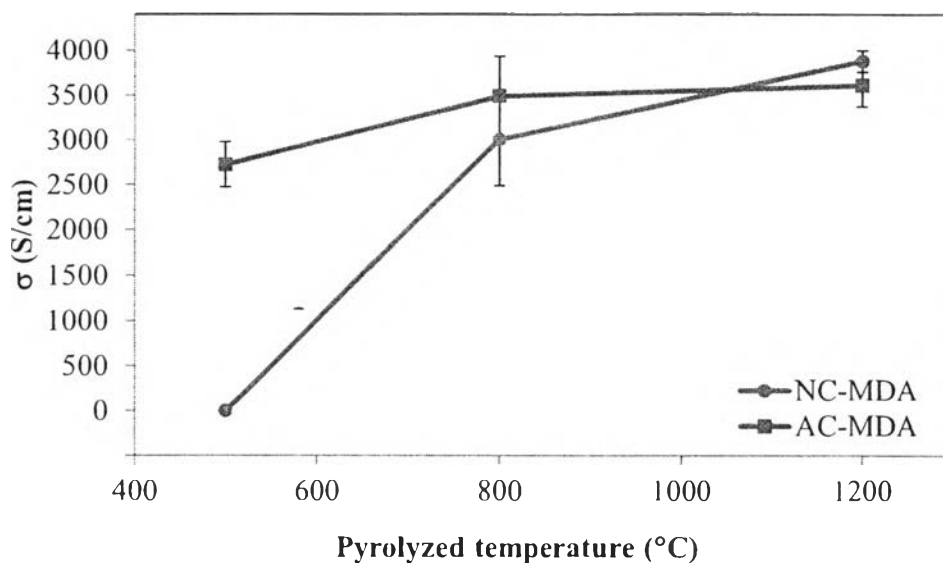
Figure 4.13 The electrical conductivities of partially ordered carbon and activated carbon with various pyrolyzed temperature.

The increasing electrical conductivities of activated carbons which were pyrolyzed at 500 and 800 °C due to the activated temperature at 900 °C as the same result that the higher temperature as a result of the creating continuous network of aromatic rings. On the other hand, the conductivity of the activated carbon, was pyrolyzed at 1200 °C, was decreased slightly comparing without activating process. Because activating process has increased the surface area and micropore volume as shown in Table 4.3 and result in the increase of the electrical conductivity owing to the created micropore as barriers which prevent the carrying electrons through the carbon to the next aromatic ring. Furthermore, the compression pressure and pyrolyzed temperature result in the increase of the electrical conductivities of partially ordered carbon due to the sp^2 carbon structures must be separated to allow any conduction path between these regions [61]. The electrical conductivity was increased due to the partially ordered carbon will be breaking, refolding into more dense packing forming closer contacts between different particles under compression pressure [62].

Conclusions

Partially ordered carbon was successfully prepared by pyrolysis process and derived from various types amine polybenzoxazine. A solventless method was used to synthesize benzoxazine precursors, then were cured in ordered to obtain completely cured polybenzoxazine. The partially ordered carbons were partially crystalline but had less crystallinity than graphite. Moreover, the ordered structure of these carbons significantly increases with temperature. The electrical conductivities increased greatly from semi-conductive to conductive materials. The activated carbon showed the significantly increasing surface area and total pore volume comparing with partially ordered carbon. When the pyrolyzed temperature is over 800 °C causing in the decrease of surface area could be due to the shrinkage of the pores and packing of carbon. The heat-treated partially ordered carbon was emphasized in conductive materials for electronic devices.

Acknowledgements

References

[1]   Fitzer, E., Kochling, K.-H. and Marsh, H.P.B.a.H. (1995). Recommended terminology for the description of carbon as a solid (IUPAC Recommendations 1995). Pure and Applied Chemistry, 67(3), 473-506.

[2]   Geim, A.K. and Novoselov, K.S. (2007). The rise of graphene. nature materials, 6, 183-191.

[3]   Novoselov, K.S., Geim, A.K., Morozov, S.V., Jiang, D., Zhang, Y., Dubonos, S.V., Grigorieva, I.V. and Firsov, A.A. (2004). Electric Field Effect in Atomically Thin Carbon Films. Science, 306(5696), 666-669.

[4]   Geim, A.K. (2009). Graphene: Status and Prospects. Science, 324(5934), 1530-1534.

[5]   Rao, C.N.R., Biswas, K., Subrahmanyam, K.S. and Govindaraj, A. (2009). Graphene, the new partially ordered carbon. Journal of Materials Chemistry, 19(17), 2457-2469.

[6]   Segal, M. (2009). Selling graphene by the ton. Nature Nanotechnology, 4(10), 612-614.

[7]   Wang, X., Zhi, L. and Mullen, K. (2007). Transparent, Conductive Graphene Electrodes for Dye-Sensitized Solar Cells. Nano Letters, 8(1), 323-327.

[8]   Stoller, M.D., Park, S., Zhu, Y., An, J. and Ruoff, R.S. (2008). Graphene-Based Ultracapacitors. Nano Letters, 8(10), 3498-3502.

[9]   Ponomarenko, L.A., Schedin, F., Katsnelson, M.I., Yang, R., Hill, E.W., Novoselov, K.S. and Geim, A.K. (2008). Chaotic Dirac Billiard in Graphene Quantum Dots. Science, 320(5874), 356-358.

[10]   Si, Y. and Samulski, E.T. (2008). Exfoliated Graphene Separated by Platinum Nanoparticles. Chemistry of Materials, 20(21), 6792-6797.

[11]   Schedin, F., Geim, A.K., Morozov, S.V., Hill, E.W., Blake, P., Katsnelson, M.I. and Novoselov, K.S. (2007). Detection of individual atmosphere molecules adsorbed on graphene. nature materials, 6(9), 652 - 655.

[12]   Stankovich, S., Dikin, D.A., Dommett, G.H.B., Kohlhaas, K.M., Zimney, E.J., Stach, E.A., Piner, R.D., Nguyen, S.T. and Ruoff, R.S. (2006). Graphene-based composite materials. Nature, 442(7100), 282-286.

[13]   Blake, P., Hill, E.W., Castro Neto, A.H., Novoselov, K.S., Jiang, D., Yang, R., Booth, T.J. and Geim, A.K. (2007). Making graphene visible. Applied Physics Letters, 91(6).

[14]   Hummers, W.S. and Offeman, R.E. (1958). Preparation of Graphitic Oxide. Journal of the American Chemical Society, 80(6), 1339-1339.

[15]   Park, S., An, J., Jung, I., Piner, R.D., An, S.J., Li, X., Velamakanni, A. and Ruoff, R.S. (2009). Colloidal Suspensions of Highly Reduced Graphene Oxide in a Wide Variety of Organic Solvents. Nano Letters, 9(4), 1593-1597.

[16] Choucair, M., Thordarson, P. and Stride, J.A. (2009). Gram-scale production of graphene based on solvothermal synthesis and sonication. <u>Nature Nanotechnology</u>, 4(1), 30-33.

[17] Hernandez, Y., Nicolosi, V., Lotya, M., Blighe, F.M., Sun, Z., De, S., McGovern, I.T., Holland, B., Byrne, M., Gun'Ko, Y.K., Boland, J.J., Niraj, P., Duesberg, G., Krishnamurthy, S., Goodhue, R., Hutchison, J., Scardaci, V., Ferrari, A.C. and Coleman, J.N. (2008). High-yield production of graphene by liquid-phase exfoliation of graphite. <u>Nature Nanotechnology</u>, 3(9), 563-568.

[18] Lotya, M., Hernandez, Y., King, P.J., Smith, R.J., Nicolosi, V., Karlsson, L.S., Blighe, F.M., De, S., Wang, Z., McGovern, I.T., Duesberg, G.S. and Coleman, J.N. (2009). Liquid Phase Production of Graphene by Exfoliation of Graphite in Surfactant/Water Solutions. <u>Journal of the American Chemical Society</u>, 131(10), 3611-3620.

[19] Reina, A., Jia, X., Ho, J., Nezich, D., Son, H., Bulovic, V., Dresselhaus, M.S. and Kong, J. (2008). Large Area, Few-Layer Graphene Films on Arbitrary Substrates by Chemical Vapor Deposition. <u>Nano Letters</u>, 9(1), 30-35.

[20] Schniepp, H.C., Li, J.-L., McAllister, M.J., Sai, H., Herrera-Alonso, M., Adamson, D.H., Prud'homme, R.K., Car, R., Saville, D.A. and Aksay, I.A. (2006). Functionalized Single Graphene Sheets Derived from Splitting Graphite Oxide. <u>The Journal of Physical Chemistry B</u>, 110(17), 8535-8539.

[21] Subrahmanyam, K.S., Vivekchand, S.R.C., Govindaraj, A. and Rao, C.N.R. (2008). A study of graphenes prepared by different methods: characterization, properties and solubilization. <u>Journal of Materials Chemistry</u>, 18(13), 1517-1523.

[22] Rao, C.N.R., Sood, A.K., Subrahmanyam, K.S. and Govindaraj, A. (2009). Graphene: The New Two-Dimensional Nanomaterial. <u>Angewandte Chemie International Edition</u>, 48(42), 7752-7777.

[23] Stankovich, S., Dikin, D.A., Piner, R.D., Kohlhaas, K.A., Kleinhammes, A., Jia, Y., Wu, Y., Nguyen, S.T. and Ruoff, R.S. (2007). Synthesis of graphene-based nanosheets via chemical reduction of exfoliated graphite oxide. <u>Carbon</u>, 45(7), 1558-1565.

[24] Andersson, O.E., Prasad, B.L.V., Sato, H., Enoki, T., Hishiyama, Y., Kaburagi, Y., Yoshikawa, M. and Bandow, S. (1998). Structure and electronic properties of graphite nanoparticles. Physical Review B, 58(24), 16387-16395.

[25] Prasad, B.L.V., Sato, H., Enoki, T., Hishiyama, Y., Kaburagi, Y., Rao, A.M., Eklund, P.C., Oshida, K. and Endo, M. (2000). Heat-treatment effect on the nanosized graphite π-electron system during diamond to graphite conversion. Physical Review B, 62(16), 11209-11218.

[26] Andersson, O.E., Prasad, B.L.V., Sato, H., Enoki, T., Hishiyama, Y., Kaburagi, Y., Yoshikawa, M. and Bandow, S. (1998). Structure and electronic properties of graphite nanoparticles. Physical Review B, 58(24), 16387-16395.

[27] Ishida, H. and Allen, D.J. (1996). Physical and mechanical characterization of near-zero shrinkage polybenzoxazines. Journal of Polymer Science Part B: Polymer Physics, 34(6), 1019-1030.

[28] Ishida, H. (2011). Chapter 1 - Overview and Historical Background of Polybenzoxazine Research. Handbook of Benzoxazine Resins. Hatsuo, I. and Tarek, A. Amsterdam, Elsevier: 3-81.

[29] Ghosh, N.N., Kiskan, B. and Yagci, Y. (2007). Polybenzoxazines—New high performance thermosetting resins: Synthesis and properties. Progress in Polymer Science, 32(11), 1344-1391.

[30] Takeichi, T., Kano, T. and Agag, T. (2005). Synthesis and thermal cure of high molecular weight polybenzoxazine precursors and the properties of the thermosets. Polymer, 46(26), 12172-12180.

[31] Agag, T. and Takeichi, T. (2003). Synthesis and Characterization of Novel Benzoxazine Monomers Containing Allyl Groups and Their High Performance Thermosets. Macromolecules, 36(16), 6010-6017.

[32] Lorjai, P., Wongkasemjit, S., Chaisuwan, T. and Jamieson, A.M. (2011). Significant enhancement of thermal stability in the non-oxidative thermal degradation of bisphenol-A/aniline based polybenzoxazine aerogel. Polymer Degradation and Stability, 96(4), 708-718.

[33] Su, Y.-C., Chen, W.-C. and Chang, F.-C. (2004). Investigation of the thermal properties of novel adamantane-modified polybenzoxazine. Journal of Applied Polymer Science, 94(3), 932-940.

[34] Ishida, H. and Krus, C.M. (1998). Synthesis and Characterization of Structurally Uniform Model Oligomers of Polybenzoxazine. Macromolecules, 31(8), 2409-2418.

[35] Křístková, M., Filip, P., Weiss, Z. and Peter, R. (2004). Influence of metals on the phenol–formaldehyde resin degradation in friction composites. Polymer Degradation and Stability, 84(1), 49-60.

[36] Al Khawwam, A., Jama, C., Goudmand, P., Dessaux, O., El Achari, A., Dhamelincourt, P. and Patrat, G. (2002). Characterization of carbon nitride layers deposited by IR laser ablation of graphite target in a remote nitrogen plasma atmosphere: nanoparticle evidence. Thin Solid Films, 408(1–2), 15-25.

[37] Li, C., Yang, X., Yang, B., Yan, Y. and Qian, Y. (2007). Synthesis and characterization of nitrogen-rich graphitic carbon nitride. Materials Chemistry and Physics, 103(2–3), 427-432.

[38] Ong, C.W., Zhao, X.A., Tsang, Y.C., Choy, C.L. and Chan, P.W. (1996). Effects of substrate temperature on the structure and properties of reactive pulsed laser deposited CNx films. Thin Solid Films, 280(1–2), 1-4.

[39] Agag, T. and Takeichi, T. (2007). High-molecular-weight AB-type benzoxazines as new precursors for high-performance thermosets. Journal of Polymer Science Part A: Polymer Chemistry, 45(10), 1878-1888.

[40] Riess, G., Schwob, J.M., Guth, G., Roche, M. and Laude, B. (1985). Ring Opening Polymerization of Benzoxazines — A New Route to Phenolic Resins. Advances in Polymer Synthesis. Culbertson, B. and McGrath, J., Springer US. 31: 27-49.

[41] Ishida, H. and Low, H.Y. (1997). A Study on the Volumetric Expansion of Benzoxazine-Based Phenolic Resin. Macromolecules, 30(4), 1099-1106.

[42] Brunovska, Z. and Ishida, H. (1999). Thermal study on the copolymers of phthalonitrile and phenylnitrile-functional benzoxazines. Journal of Applied Polymer Science, 73(14), 2937-2949.

[43] Liu, J., Agag, T. and Ishida, H. (2011). Chapter 18 - Main-Chain Type Benzoxazine Oligomers: A New Concept for Easy Processable High Performance Polybenzoxazines. Handbook of Benzoxazine Resins. Hatsuo, I. and Tarek, A. Amsterdam, Elsevier: 355-362.

[44] Lu, G.Q., Low, J.C.F., Liu, C.Y. and Lua, A.C. (1995). Surface area development of sewage sludge during pyrolysis. Fuel, 74(3), 344-348.

[45] Lin, Q., Dong, S., Qu, L., Fang, C. and Luo, K. (2014). Preparation and properties of carbon foam by direct pyrolysis of ally novolak-modified bismaleimide resin. Journal of Analytical and Applied Pyrolysis, 106(0), 164-170.

[46] Lü, Q.-F., He, Z.-W., Zhang, J.-Y. and Lin, Q. (2011). Preparation and properties of nitrogen-containing hollow carbon nanospheres by pyrolysis of polyaniline–lignosulfonate composites. Journal of Analytical and Applied Pyrolysis, 92(1), 152-157.

[47] Lin, Q., Tang, H., Guo, D. and Zheng, M. (2010). Preparation and properties of carbon microbeads by pyrolysis of N-phenyl maleimide modified novolac resin. Journal of Analytical and Applied Pyrolysis, 87(2), 276-281.

[48] Chen, Y., Chen, B.-Z., Shi, X.-G., Xu, H., Hu, Y.-J., Yuan, Y. and Shen, N.-B. (2007). Preparation of pitch-based carbon foam using polyurethane foam template. Carbon, 45(10), 2132-2134.

[49] Wu, D., Fu, R. and Yu, Z. (2005). Organic and carbon aerogels from the NaOH-catalyzed polycondensation of resorcinol–furfural and supercritical drying in ethanol. Journal of Applied Polymer Science, 96(4), 1429-1435.

[50] Zhu, S., Su, C.-H., Cochrane, J.C., Lehoczky, S., Muntele, I. and Ila, D. (2001). Growth of carbon nanostructure materials using laser vaporization. Diamond and Related Materials, 10(3–7), 1190-1194.

[51] Morjan, I., Voicu, I., Dumitrache, F., Sandu, I., Soare, I., Alexandrescu, R., Vasile, E., Pasuk, I., Brydson, R.M.D., Daniels, H. and Rand, B. (2003). Carbon nanopowders from the continuous-wave CO2 laser-induced pyrolysis of ethylene. Carbon, 41(15), 2913-2921.

[52] Mrozowski, S. (1979). Specific heat anomalies and spin-spin interactions in carbons: A review. Journal of Low Temperature Physics, 35(3-4), 231-298.

[53] Machnikowski, J., Rutkowski, P. and Diez, M.A. (2006). Co-treatment of novolac- and resole-type phenolic resins with coal-tar pitch for porous carbons. Journal of Analytical and Applied Pyrolysis, 76(1–2), 80-87.

[54] Zhang, T., Walawender, W.P., Fan, L.T., Fan, M., Daugaard, D. and Brown, R.C. (2004). Preparation of activated carbon from forest and agricultural residues through CO2 activation. Chemical Engineering Journal, 105(1–2), 53-59.

[55] Rodríguez-Reinoso, F. and Molina-Sabio, M. (1992). Activated carbons from lignocellulosic materials by chemical and/or physical activation: an overview. Carbon, 30(7), 1111-1118.

[56] Lua, A.C. and Guo, J. (2001). Microporous Oil-Palm-Shell Activated Carbon Prepared by Physical Activation for Atmosphere-Phase Adsorption. Langmuir, 17(22), 7112-7117.

[57] Diakoumakos, C.D., Mikroyannidis, J.A., Krontiras, C.A., Pisanias, M.N. and Georga, S.N. (1995). Thermosetting resins prepared from the reactions of diaminomaleonitrile with 4,4'-bismaleimidediphenylmethane and electrical conductivity measurements of the resulting materials following pyrolysis. European Polymer Journal, 31(11), 1057-1066.

[58] Sánchez-González, J., Stoeckli, F. and Centeno, T.A. (2011). The role of the electric conductivity of carbons in the electrochemical capacitor performance. Journal of Electroanalytical Chemistry, 657(1–2), 176-180.

[59] Kennedy, L.J., Vijaya, J.J. and Sekaran, G. (2005). Electrical conductivity study of porous carbon composite derived from rice husk. Materials Chemistry and Physics, 91(2–3), 471-476.

[60] Wang, L., Wang, X., Zou, B., Ma, X., Qu, Y., Rong, C., Li, Y., Su, Y. and Wang, Z. (2011). Preparation of carbon black from rice husk by hydrolysis, carbonization and pyrolysis. Bioresource Technology, 102(17), 8220-8224.

[61] Racine, B., Benlahsen, M., Zellama, K., Bouzerar, R., Kleider, J.P. and Von Bardeleben, H.J. (2001). Electronic properties of hydrogenated amorphous carbon films deposited using ECR-RF plasma method. Diamond and Related Materials, 10(2), 200-206.

[62] Mrozowski, S. (1958). Studies of carbon powders under compression I. Proceedings of The 3rd Conference on Carbon, Symposium Publications Division, Pergamon Press.